JOURNAL OF GEOPHYSICAL RESEARCH, VOL. 103, NO. D17, PAGES 22,115-22,127, SEPTEMBER 20, 1998

Two new methods for deriving tropospheric column ozone from TOMS measurements: Assimilated UARS MLS/HALOE and convective-cloud differential techniques

J. R. Ziemke[1]
Software Corporation of America, Lanham, Maryland

S. Chandra and P. K. Bhartia
NASA Goddard Space Flight Center, Greenbelt, Maryland

Abstract. This study introduces two new approaches for determining tropospheric column ozone from satellite data. In the first method, stratospheric column ozone is derived by combining Upper Atmosphere Research Satellite (UARS) halogen occultation experiment (HALOE) and microwave limb sounder (MLS) ozone measurements. Tropospheric column ozone is then obtained by subtracting these stratospheric amounts from the total column. Total column ozone in this study include retrievals from Nimbus 7 (November 1978 to May 1993) and Earth probe (July 1996 to present) total ozone mapping spectrometer (TOMS). Data from HALOE are used in this first method to extend the vertical span of MLS (highest pressure level 46 hPa) using simple regression. This assimilation enables high-resolution daily maps of tropospheric and stratospheric ozone which is not possible from solar occultation measurements alone, such as from HALOE or Stratospheric Aerosols and Gas Experiment (SAGE). We also examine another new and promising technique that yields tropospheric column ozone directly from TOMS high-density footprint measurements in regions of high convective clouds. We define this method as the convective cloud differential (CCD) technique. The CCD method is shown to provide long time series (essentially late 1978 to the present) of tropospheric ozone in regions dominated by persistent high tropopause-level clouds, such as the maritime tropical Pacific and within or near midlatitude continental landmasses. In this our first study of the CCD and MLS/HALOE methods we limit analyses to tropical latitudes. Separation of stratospheric from tropospheric column ozone in the eastern Pacific tropics for January 1979 to December 1997 shows that the dominant interannual variability of stratospheric ozone is the quasi-biennial oscillation (QBO), whereas for tropospheric ozone it is driven by El Niño events. For validation purposes, both the CCD and assimilated UARS MLS/HALOE results are compared with ozonesonde data from several southern tropical stations. Despite all three measurements being distinctly different in sampling and technique, all three show good qualitative agreement.

1. Introduction

The study by *Fishman and Larsen* [1987] was the first to derive tropospheric column ozone from satellite data by combining Stratospheric Aerosols and Gas Experiment (SAGE) stratospheric column ozone with total ozone mapping spectrometer (TOMS) total ozone measurements. This approach, which subtracts SAGE stratospheric column ozone from TOMS total column ozone, is called the tropospheric ozone residual (TOR) method. The study by *Fishman and Larsen* [1987] and subsequent studies, including *Fishman et al.* [1992, 1996], revealed an anomalous zonal pattern in tropospheric column ozone in the tropics with a characteristic peak in the south Atlantic region. A number of studies have indicated that ozone production triggered by biomass burning, specifically over South America and Africa, has an important role in the formation of the south Atlantic anomaly [e.g., *Fishman et al.*, 1996, and

[1]Also at NASA Goddard Space Flight Center, Greenbelt, Maryland.

Paper number 98JD01567.
0148-0227/98/98JD-01567$09.00

references therein; *Jacob et al.*, 1996; *Thompson et al.*, 1996]. However, the interpretation of the tropical ozone anomaly is complicated by the fact that several meteorological parameters also show a predominant yearround zonal wave 1 structure similar to tropospheric ozone, thus raising the possibility that the horizontal background distribution of tropospheric ozone in the tropics is generated largely by natural meteorological conditions [*Krishnamurti et al.*, 1993, 1996; *Ziemke et al.*, 1996; *Ziemke and Chandra*, 1998a]. *Krishnamurti et al.* [1993, 1996] showed that tropospheric subsidence and horizontal transport of air in the south Atlantic during October months can produce an ozone peak in this region even without the presence of tropospheric ozone production from biomass burning. It is apparent that an understanding of dynamical and biogenic sources in the tropical troposphere requires a detailed characterization of temporal and spatial variabilities in order to delineate the relative importance of these processes.

The use of SAGE data in deriving tropospheric ozone, though useful, has an important disadvantage. SAGE is a solar occultation instrument, restricting daily coverage to only two (sunrise and sunset) narrow 5°-10° latitude bands. This poor sampling of data seriously limits the interpretation of tropospheric column ozone maps from daily to monthly timescales. To alleviate this problem, *Fishman et al.* [1996] and *Vukovich et al.* [1996] combined Nimbus 7 TOMS total ozone with vertical ozone profiles from the NOAA 11 Solar Backscatter Ultraviolet 2 (SBUV2) instrument in an effort to better determine tropical TOR maps. TOR was calculated by subtracting SBUV2 stratospheric column ozone from TOMS total ozone. Using the TOMS-SBUV2 combination to derive TOR in both studies appeared to be an improvement from using TOMS-SAGE as by *Fishman et al.* [1992]. In contrast to SAGE, SBUV2 is a polar orbiting and nadir (straight downward) viewing instrument and makes approximately 14 orbits per day, providing daily coverage over much of the Earth (excluding polar night latitudes). However, as pointed out by *Ziemke and Chandra* [1998b], ozone profiles from SBUV depend critically on the shape of SBUV vertical weighting functions, and below the ozone number density peak (around 20 to 25 km altitude) there are serious retrieval errors. Direct application of SBUV to derive tropospheric ozone will have persistent algorithmic errors.

A detailed characterization of the temporal and spatial variability of tropospheric ozone thus requires new and unique approaches. Recently, *Hudson and Thompson* [1998] have developed a modified residual method that combines TOMS total ozone with ground-based ozonesonde measurements. In our study we introduce two new and promising methods. The first combines TOMS total ozone with Upper Atmosphere Research Satellite (UARS) microwave limb sounder (MLS) and halogen occultation experiment (HALOE) stratospheric ozone data. Our second method requires only high-density footprint measurements of TOMS total ozone and reflectivity in regions of high tropopause-level clouds. We define this as the convective cloud differential (CCD) technique. The CCD method utilizes the fact that in such regions, high-reflectivity cases are often associated with strong convection and cloud tops near the tropopause, as indicated by *Eck et al.* [1987] and *Stowe et al.* [1988, 1989]; each of these studies compared TOMS reflectivity measurements with concurrent temperature humidity infrared radiometer (THIR) 11.5-μm cloud top pressures.

An important property of the TOMS CCD method is that it does not require other satellite ozone measurements, such as from UARS MLS, HALOE, or from SAGE. Both CCD and assimilated UARS MLS/HALOE procedures will be shown to be viable alternative techniques.

2. Data

Satellite ozone profile data used in this study include UARS version 18 HALOE and version 4 205-GHz MLS volume mixing ratio measurements for September 1991 through September 1997. Validation of HALOE has been discussed by *Brühl et al.* [1996], and similar validation of MLS is discussed by *Froidevaux et al.* [1996]. All MLS and HALOE data used in this study were binned to 5°latitude (85°S to 85°N) × 15°longitude blocks for analysis.

Data from HALOE are included in this investigation in effort to extend the vertical span of MLS (highest pressure level 46 hPa) using a linear regression approach (discussed later). This assimilation enables the construction of high horizontal resolution daily maps of stratospheric ozone which is not possible using solar occultation measurements from either SAGE or UARS HALOE alone. TOMS data from Nimbus 7 (N7) for 1979-1992 and Earth probe (EP) for July 1996 to December 1997 were used in our study to provide high-density footprint measurements of total column ozone and effective reflectivity. Meteor 3 TOMS from late August 1991 to December 1994 bridges the temporal gap beween Nimbus 7 and EP TOMS time periods and represents another important data source. However, Meteor 3 TOMS data were not included in our study because of a non-Sun-synchronous orbit where even tropical measurements exhibit high solar zenith angles which greatly affects results from the CCD method. Effective footprint diameter size for N7 TOMS at nadir is ~50 km and around 200 km in the extreme off-nadir direction. In comparison, because of a lower orbit (~500 km altitude), these numbers for EP TOMS are ~25 and 100 km, respectively. (In December 1997, EP TOMS was raised to a higher orbit (~750 km) increasing footprint size to nearly that of N7 TOMS.) Further information regarding TOMS instruments can be obtained via the World Wide Web TOMS homepage (currently, http://jwocky.gsfc.nasa.gov/#TOMS_Data).

Ozonesonde measurements (1978-1996) from southern tropical stations Brazzaville (4°S, 15°E; 1991-1992), Ascension Island (8°S, 15°W; 1991-1992), Natal (5°S, 35°W; 1978-1992), and Samoa (14°S, 170°W; 1986-1990

and 1995-1996) are used to help validate results for both the CCD and assimilated UARS MLS/HALOE methods introduced in this study. For determining tropospheric column ozone from the sonde data, the tropopause is inferred from coincident sonde measurements of temperature profiles.

3. Combined TOMS and UARS MLS/HALOE Ozone

Data from HALOE are used in this study to extend the vertical span of MLS (highest-pressure level 46 hPa) down to the tropopause in the tropics using standard regression. In this method we assume as a first approximation that the variability in the vertical structure of ozone lying between the lowest derived altitude from MLS (46 hPa) and the tropopause is correlated with the ozone column above 46 hPa. Stratospheric column ozone (Ω_S) in the stratosphere is derived from $\Omega_S = \gamma\Omega_{0-46hPaMLS} + \epsilon$, where ϵ is the residual error and Ω_S in the regression is taken from HALOE overpass ozone, relative to MLS. Coefficient γ was derived at each latitude by regressing daily stratospheric column ozone amounts from HALOE onto 0-46 hPa MLS column ozone from January 1993 through December 1996. These daily regression coefficients were then averaged monthly for this study. (Further details regarding the derivation of γ and statistical analyses are discussed in the appendix.) For calculating tropospheric column ozone, tropopause pressure was interpreted from National Centers for Environmental Prediction (NCEP) temperature analyses. We note that errors in tropopause pressure translate directly to errors in tropospheric column ozone, but the effect is generally small in low latitudes. In the tropics, upper bound uncertainties of 20 hPa (1-1.5 km) about the true tropopause pressure produce errors of around 2 DU, and up to ~5 DU in column ozone as inferred from ozonesonde temperature and ozone profiles in the Pacific and Atlantic regions, respectively. In this study, we focus only on tropical latitudes 20°S to 20°N.

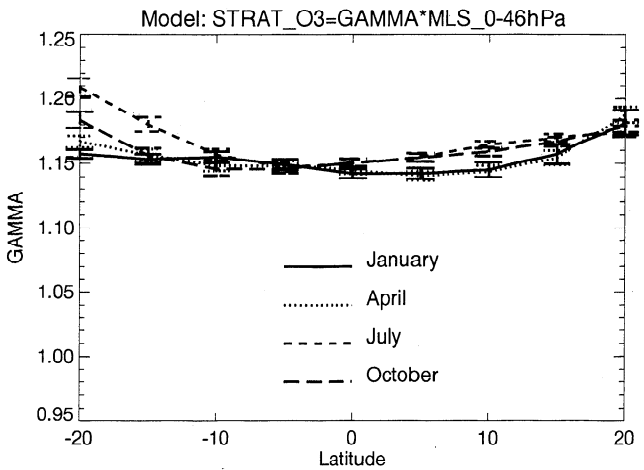

Figure 1. Monthly-averaged (selected months shown) regression coefficient γ plotted versus latitude. Included are $\pm 2\sigma$ error bars in γ (see appendix).

Figure 1 shows coefficient γ for the selected months of January, April, July, and October. Also included are regression error bars for ± 2 standard deviations ($\pm 2\sigma$). The combination of both seasonal and latitudinal variabilities of γ in the tropics indicates relatively sizable changes of up to 5% and exceed the statistical $\pm 2\sigma$ uncertainties that are closer to $\pm 1\%$. Typical 0-46 hPa column ozone in the tropics calculated from MLS measurements is around 200 DU so that $5\% \pm 1\%$ variability of γ generates approximately 10 ± 2 DU variability in computed stratospheric column ozone.

The monthly and latitudinally varying coefficient γ was applied to September and October 1996 monthly mean 0-46 hPa column ozone from MLS, as shown in Plate 1. Consistent with the studies by *Fishman et al.* [1992] and *Ziemke et al.* [1996], tropospheric ozone indicates a dominant zonal wave 1 variability with largest values ~40-50 Dobson units (DU) in the south Atlantic region. Smallest ozone amounts occur in the western Pacific and coincide with a region of strong convection. Effects from the Andes (2-6 km altitudes) running along the western coast of South America produce up to 10-15 DU depressions in tropospheric ozone.

Comparisons between tropospheric ozone from the UARS MLS/HALOE method and that of concurrent ozonesondes at Ascension Island and Brazzaville are shown in Figure 2. Similar comparisons for Natal and Samoa were not possible for this time period because of a lack of sufficient ozonesonde data (none for Samoa). Despite being distinctly different in both technique and sampling (some months shown for ozonesondes have only one ozone profile), there is nevertheless a good qualitative agreement with respect to the seasonal cycle at Acsension Island, but less so at Brazzaville. In the next section we will investigate a different approach for deriving tropospheric column ozone directly from TOMS measurements.

4. Convective Cloud Differential Technique

The CCD technique is depicted in the schematic diagram shown in Figure 3. In the top frame, total ozone is computed for low reflectivity ($R < 0.2$, left) while stratospheric column ozone is determined from nearby total ozone measurements taken above the tops of very high clouds for high reflectivity ($R > 0.9$, right). Because TOMS cannot detect ozone below cloud top heights, the algorithm places a predetermined best guess amount of column ozone below the cloud. This amount is subtracted from total ozone in determining the ozone column above the cloud. We note that other critical values of reflectivity were tested, indicating that 0.2 and 0.9 are good choices that work well for N7 and EP TOMS footprint measurements.

Figure 3 (bottom) indicates that the high-reflectivity clouds viewed by TOMS are sometimes associated with cloud tops lying below the tropopause, resulting in an

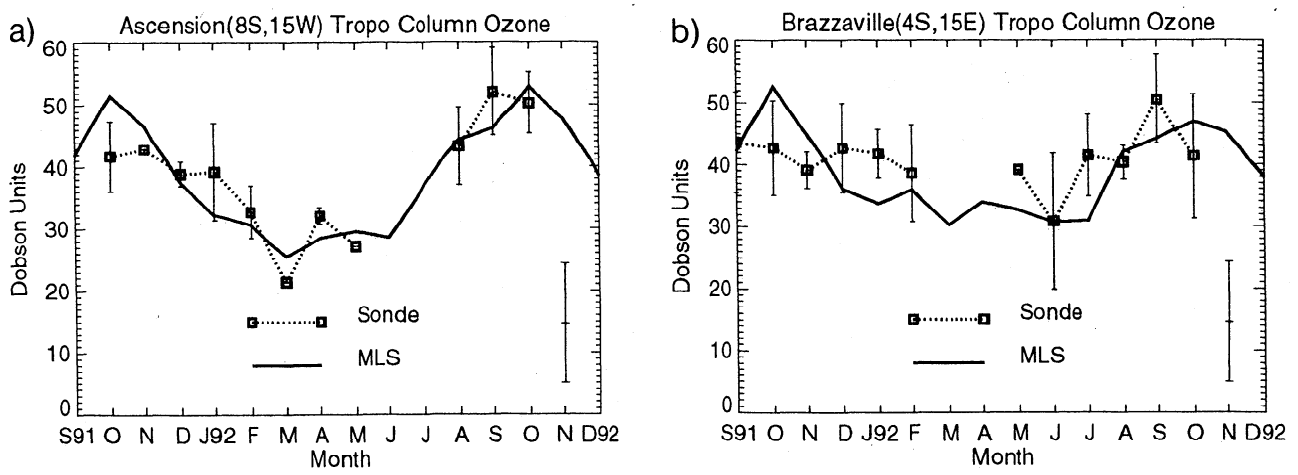

Figure 2. Monthly mean tropospheric column ozone measurements from the UARS MLS/HALOE method (solid) plotted along with concurrent ozonesondes measurements (boxes): (a) Ascension Island (8°S, 15°W) and (b) Brazzaville (4°S, 15°E). Included for ozonesonde measurements are $\pm 1\sigma$ uncertainty bars calculated from all available daily data within a given month; bars for months with only one sonde measurement are identically zero. For the MLS/HALOE time series, monthly errors are represented by the $\pm 2\sigma$ (i.e., ± 10 DU) error bar plotted in the lower right portion of each frame.

over-estimation of stratospheric column ozone. One procedure to alleviate this difficulty is to use only the smallest derived stratospheric column measurements. Another approach is statistical, using ensemble means and standard deviations. Results using both of these methods will be presented below. In this first study of the CCD method, statistical variables (footprint counts, means, standard deviations, and extreme values) were binned to a monthly 5° by 5° latitude-longitude framework for analysis.

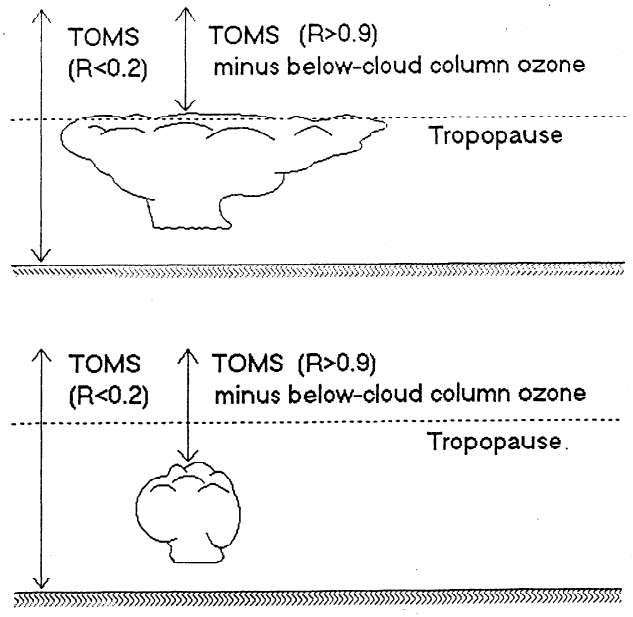

Figure 3. Schematic illustration of the CCD technique. (top) Tropospheric ozone is computed by taking total ozone with low reflectivity ($R < 0.2$) and subtracting from this a nearby measurement of total ozone with high reflectivity ($R > 0.9$) (after removing below-cloud column amount). (bottom) Not all high-reflectivity cases viewed by TOMS are associated with cloud tops near the tropopause.

4.1. Cloud Tops

Because the CCD method requires high tropopause-level cloud tops, an important preliminary question to answer is the following: in what regions of the globe are convective clouds most often associated with cloud tops near the tropopause? To answer this, we incorporated monthly mean cloud top pressure data from International Satellite Cloud Climatology Project (ISCCP) [*Rossow and Garder*, 1993] (Figure 4).

Regardless of geographical location, monthly mean cloud top pressures will generally indicate altitudes that are several hundred hPa below the tropopause. For example, in the tropics the tropopause lies around 100 hPa everywhere, but ISCCP data indicate monthly mean cloud top pressures around 400-500 hPa in the highly convective tropical western Pacific and around 600-800 hPa in the eastern Pacific (not shown in Figure 4). In addition, corresponding temporal standard deviations in a given month from ISCCP indicate amplitudes ~150 hPa in the western Pacific and ~100 hPa in the eastern Pacific. Hence cloud tops have considerable variability, both spatially and temporally, and plotting only monthly mean cloud top pressures for example will not provide information on the frequency of occurrence of tropopause-level cloud tops. In this study we employed a statistical scheme to identify regions that have the highest frequency of tropopause-level cloud tops. For each month of ISCCP data we subtracted two

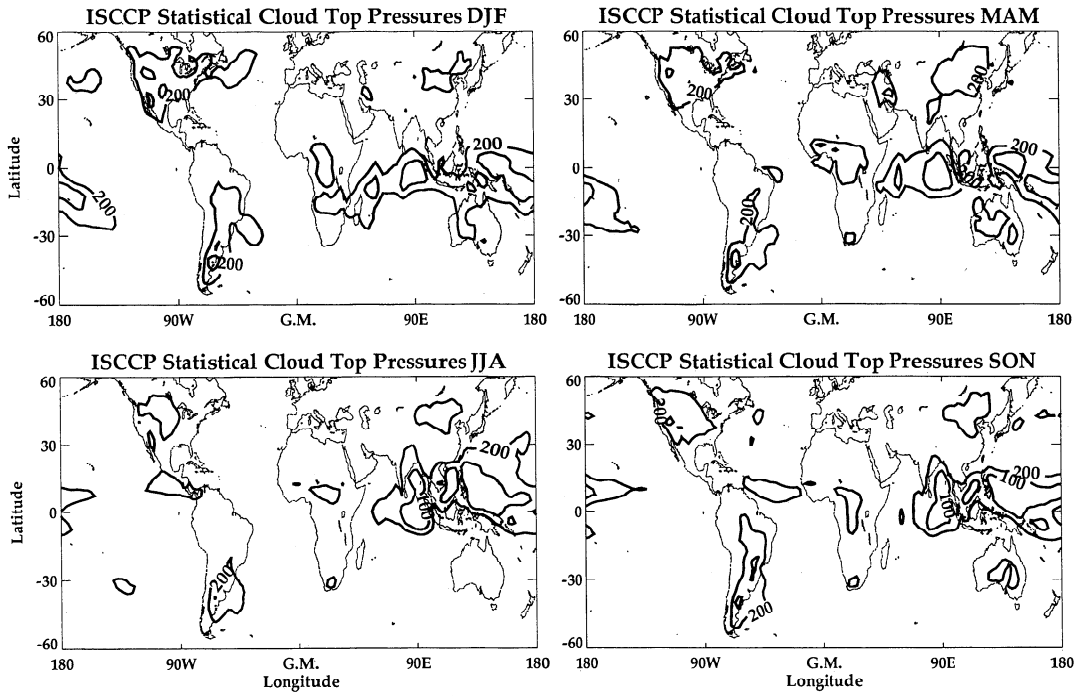

Figure 4. Statistical cloud top pressures (in hPa) derived from Internatinal Satellite Cloud Climatology Project (ISCCP) for the time period 1984-1990. Pressures were determined statistically by subtracting two temporal standard deviations (2σ) from monthly means, followed by averaging within 3-month seasons (indicated). Contours plotted are 100 and 200 hPa. (Monthly means and standard deviations were provided by D. Larko (personal communication, 1997).)

temporal standard deviations (2σ) from monthly mean cloud top pressures. This subtraction identifies roughly the 2.5% probability tail of lowest-pressure (highest-altitude) cases, thus indicating regions that have the greatest frequency of tropopause-level cloud tops.

Shown in Figure 4 are these computed statistical cloud top pressures, averaged seasonally (indicated) over similar months for January 1984 to December 1990. Because the tropopause lies around 100 hPa in the tropics, Figure 4 shows that the tropical western Pacific is where we have the greatest frequency of tropopause-level cloud tops. It is expected then that the CCD method will work best in this region. We note that Figure 4 also indicates midlatitude regions where clouds often reach and exceed the tropopause ($\sim 170 \pm 50$ hPa), such as North America, southeast South America, and the eastern portion of the Asian continent. In this first study of the CCD method, we will limit our analyses to only the tropical latitudes.

4.2. Tropospheric Ozone Derived From EP TOMS

As our first example of the CCD technique, Figure 5 shows total ozone (dense dots) and above cloud top estimated stratospheric ozone (plus symbols) derived from EP TOMS for October 30-31, 1996. The large variability present in total ozone reflects the natural variability present within the 10°S-5°N latitudinal band. We note that some of these total ozone measurements are affected by a well-known scan-angle artifact present in TOMS measurements [*McPeters et al.*, 1996], but the impact of this artifact is small; high side scan angles produce around 1-3 DU over-determination of total ozone which is noise level for TOMS. The above cloud top column ozone also shows significant variability caused by natural variability in cloud top pressures.

Also present in Figure 5 are independent stratospheric column ozone integrations from HALOE between 0 and 100 hPa (100 hPa is approximately the tropopause pressure), and MLS column ozone for 0-46 hPa; MLS in Figure 5 includes a +25 DU offset that brings this curve up to that of HALOE for visual comparison. Both HALOE and MLS indicate a generally zonally invariant stratospheric column amount, and is similar to the CCD method despite the fact that cloud tops reach the tropopause consistently only in the Pacific region west of the dateline (see Figure 4). Comparison with tropical ozonesonde station locations in the Atlantic region (Natal, Ascension Island, Brazzaville) indicates that the direct CCD method in general provides relatively few data values, as high-reflectivity footprint events are more sparse, and cloud tops are less apt to reach the tropopause. A way around this difficulty is to assume to first-order a zonally invariant stratospheric ozone column in low latitudes as indicated in Figure 5 for MLS and HALOE integrations. It will be shown later that this first-order assumption well reproduces seasonal and longer timescale variabilities observed by ozonesonde measurements at these tropical stations.

Plate 2 shows September and October 1996 tropo-

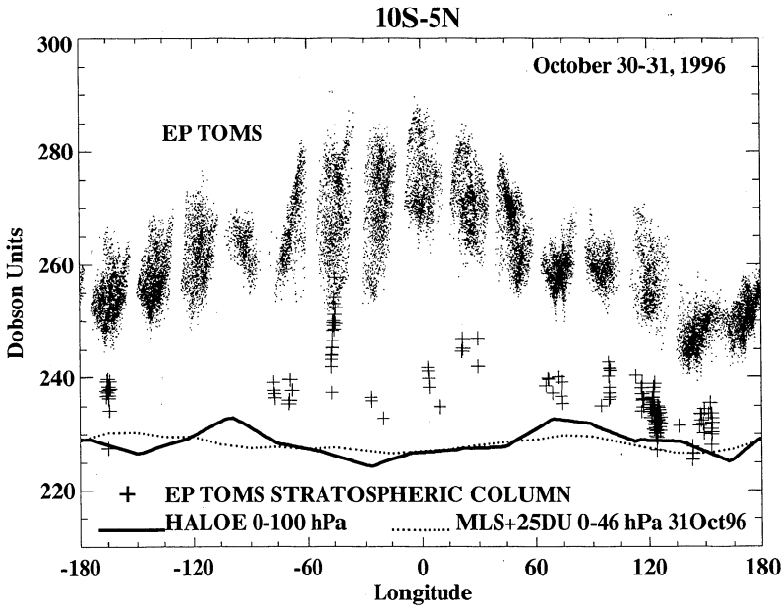

Figure 5. Longitude lineplot of high-density footprint measurements of EP TOMS total ozone (thick dots), UARS HALOE 0-100 hPa stratospheric column ozone (solid), UARS MLS 0-46 hPa stratospheric column ozone for October 31, 1996 (dotted), and stratospheric column ozone derived from the EP TOMS footprint data using the CCD method (plus symbols). Cloud (high-reflectivity case) assumed a minimum reflectivity of 0.9, while no-cloud (low-reflectivity case) assumed a maximum reflectivity of 0.2. All available data were averaged between 10°S to 5°N for October 30-31, 1996. MLS column ozone was given a +25 DU offset to bring it up alongside the HALOE curve; MLS data were not available for October 30, 1996.

spheric column ozone estimated from the CCD method, where we have assumed zonal invariance of stratospheric column ozone. Stratospheric column ozone was derived at each latitude by averaging data (minimum values of estimated stratospheric column ozone) from 120°E eastward to the dateline. Comparison of Plate 2 with Plate 1 shows that the assumption of a zonally invariant stratospheric ozone column produces a similar zonal wave 1 pattern with amplitudes around 40-50 DU in the south Atlantic and lower values ~20 DU in the western Pacific. Smaller-scale topographic effects are again evident such as the South American Andes and the mountainous region of southern Africa. A closer examination of Plates 1 and 2 indicates that the MLS/HALOE column amounts are smaller by ~5 DU in the lowest latitudes and may be a result of intercalibration differences between these various instruments. On average, TOMS CCD minus MLS/HALOE tropospheric column amounts during the July 1996 to December 1997 EP TOMS time period throughout the tropics were found to be consistently positive by ~4-5 DU while during the September 1991-April 1993 Nimbus 7 overlapping time period differences where negative by ~3-4 DU. Despite the fact that both the CCD and MLS/HALOE methods provide similar maps with similar column amounts, further improvements of both methods (beyond the scope of the present study) including intercalibration issues will be necessary to resolve smaller temporal and spatial variabilities. In the following section we will derive long continuous time series (1979-1992) of tropospheric ozone in the tropics using the CCD method.

4.3. Tropospheric Column Ozone for 1979-1992

We next examine the properties of tropospheric ozone in the tropics using the CCD method and 1979-1992 N7 TOMS data. Rather than assume that the best estimates of stratospheric column ozone from the CCD method are derived using only minimum values within a given 5° × 5° bin (as was used in Plate 2), we instead applied a statistical approach where the absolute minimum accepted number of footprints with $R > 0.9$ in any 5° × 5° monthly bin must exceed 10. Stratospheric column ozone was then determined statistically by taking the mean and subtracting from this two standard deviations. Although differences in derived stratospheric column ozone between these two methods were found to be small, this statistical approach may be more accurate since it involves ensemble averaging. This latter method was invoked for the remainder of all of our CCD results presented in this study. In this first study of the CCD approach we investigated several alternative averaging schemes, including that of averaging data further eastward across the dateline to 120°W encompassing El Niño months. We note that during El Niño there is a shift of large-scale convection into the eastern Pacific and the CCD method can benefit by including these high cloud tops as well as those in the western Pacific.

Average seasonal counts (number of N7 TOMS footprints) with $R > 0.9$ for 1979-1992 are shown in Figure 6. Most high-reflectivity cases lie along the intertropical convergence zone (ITCZ), maximizing in the Indian Ocean-western Pacific region. In mid-high latitudes,

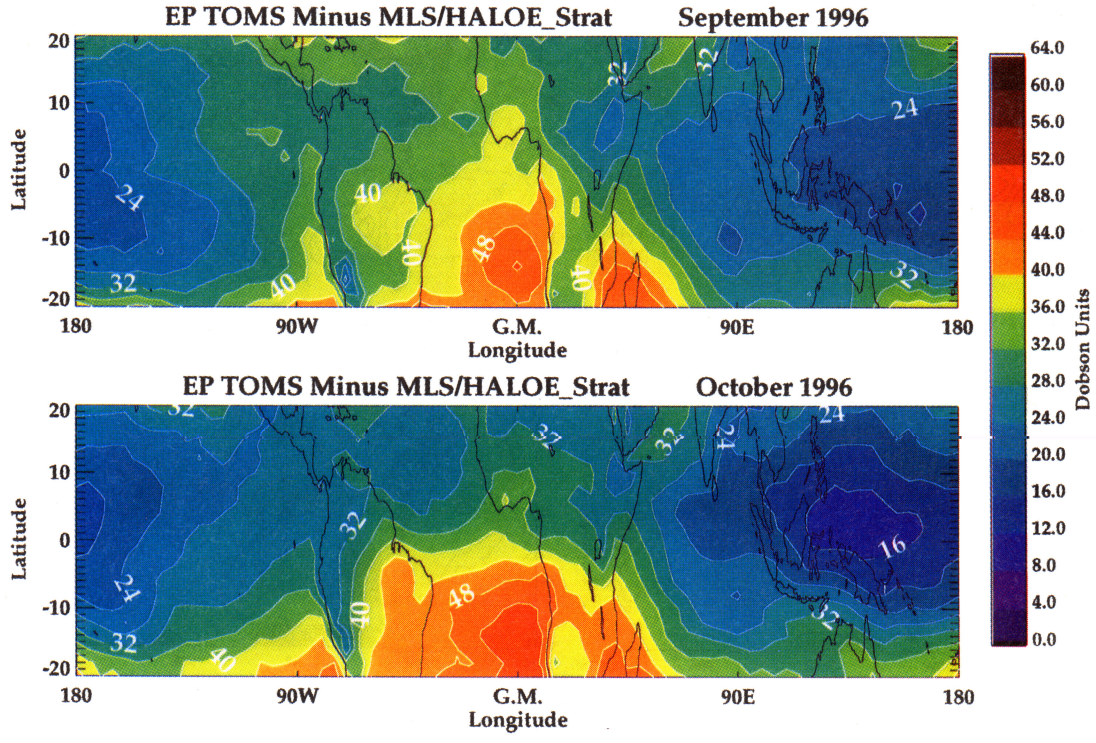

Plate 1. Tropical tropospheric column ozone (in Dobson units) for (top) September and (bottom) October 1996 computed from the MLS/HALOE assimilation method. Local 2σ errors are estimated (see appendix) to be 10 DU.

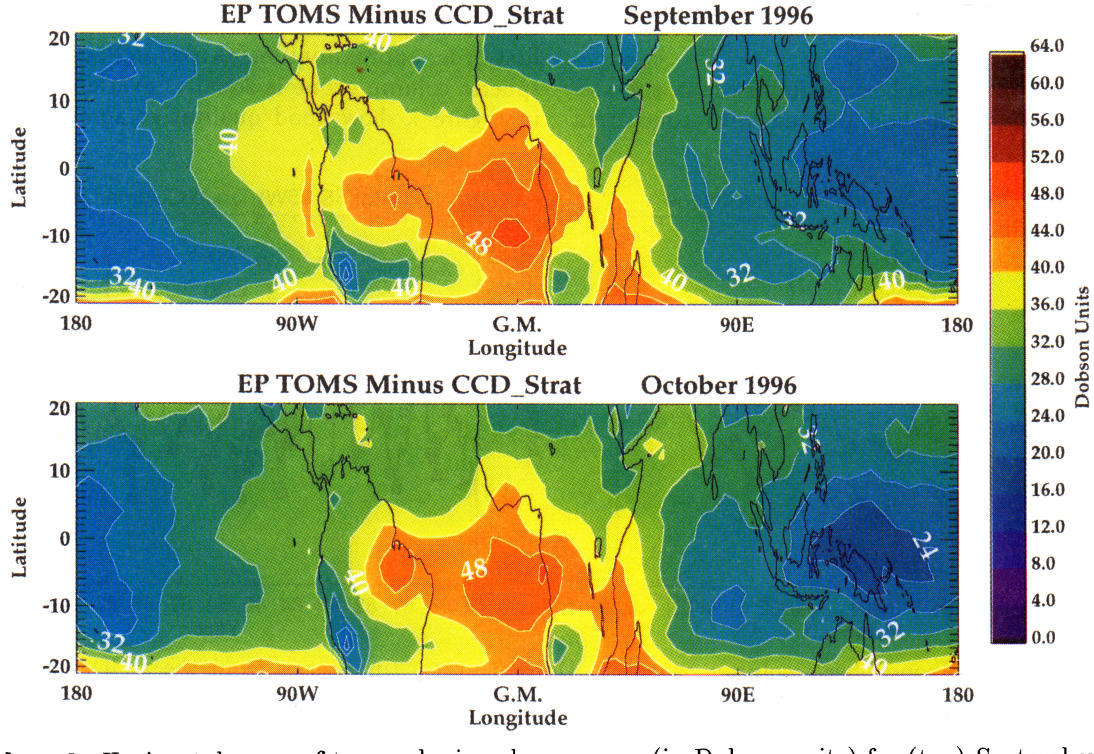

Plate 2. Horizontal maps of tropospheric column ozone (in Dobson units) for (top) September and (bottom) October 1996 computed from the CCD technique. Local 2σ errors are estimated (see appendix) to be 7 DU.

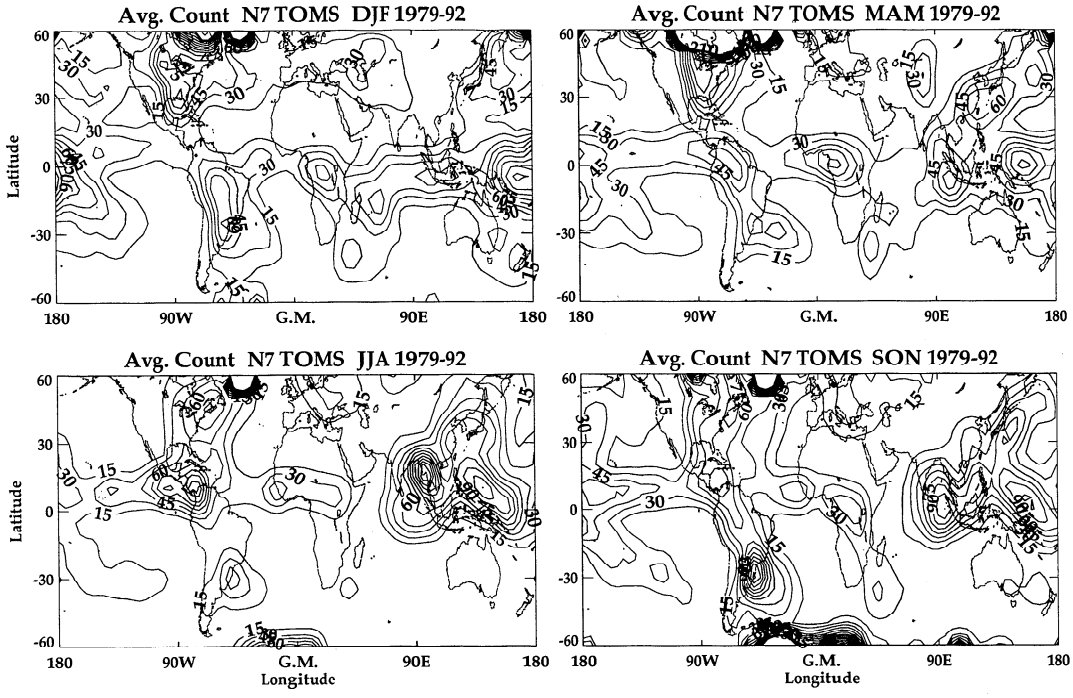

Figure 6. Climatological (1979-1992) average number of N7 TOMS footprints within 3-month seasons (DJF, MAM, JJA, SON, indicated) having reflectivity $R > 0.9$.

especially in winter-spring months, high-reflectivity regions also indicate snow and ice. In this study we focus on tropical latitudes, although other midlatitude regions in Figure 6 (noted previously in Figure 4) such as North America, southeast South America, and east Asia, also experience persistent high tropopause-level clouds.

Figure 7 shows tropospheric column ozone time series from the CCD method plotted with concurrent ozonesonde measurements from Ascension Island (left) and Natal (right). Because cloud tops in the tropics away from the highly convective Indian Ocean-western Pacific region are less apt to reach the tropopause on average (and there are fewer high reflectivity TOMS cases), time series in Figure 7 were derived using the first-order approximation (as used in Plate 2) that stratospheric column ozone is zonally invariant. Time series in Figure 7 show good qualitative agreement, despite

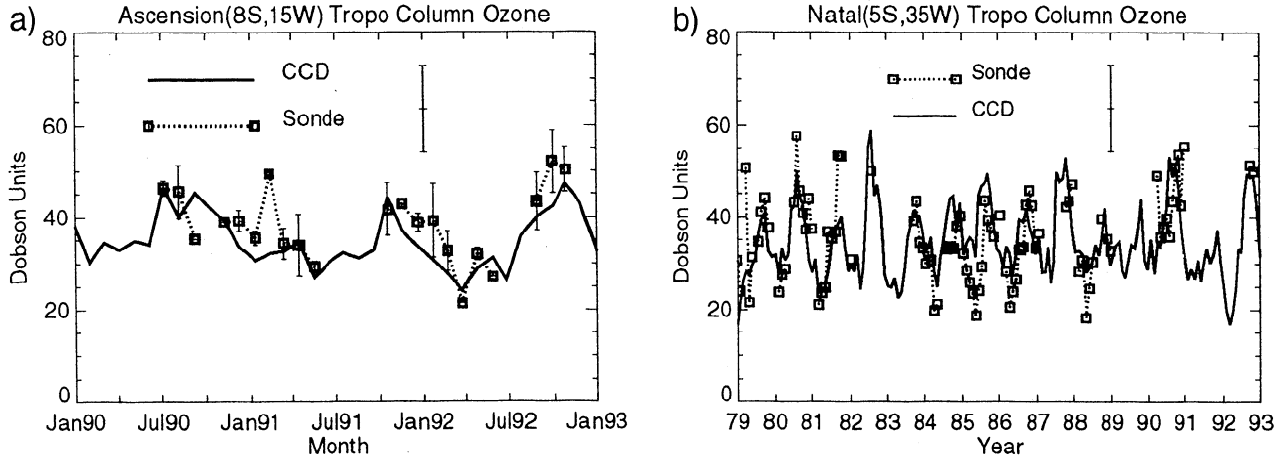

Figure 7. Tropospheric column ozone (in Dobson units) time series from the CCD method plotted with concurrent ozonesonde measurements from (a) Ascension Island (8°S, 15°W), and (b) Natal (5°S, 35°W). Time series for the CCD method were derived using the statistical 2σ method (see section 4), and assumed the first-order approximation that the stratospheric ozone column is zonally invariant. Included for Ascension Island ozonesonde measurements are $\pm 1\sigma$ uncertainty bars calculated from all available daily data within a given month; bars for months with only one sonde measurement are identically zero. For clarity, uncertainty bars for Natal sonde data are not plotted. Monthly $\pm 2\sigma$ (i.e., ± 7 DU) errors for CCD time series are represented by the vertical bar plotted in the top right portion of each frame.

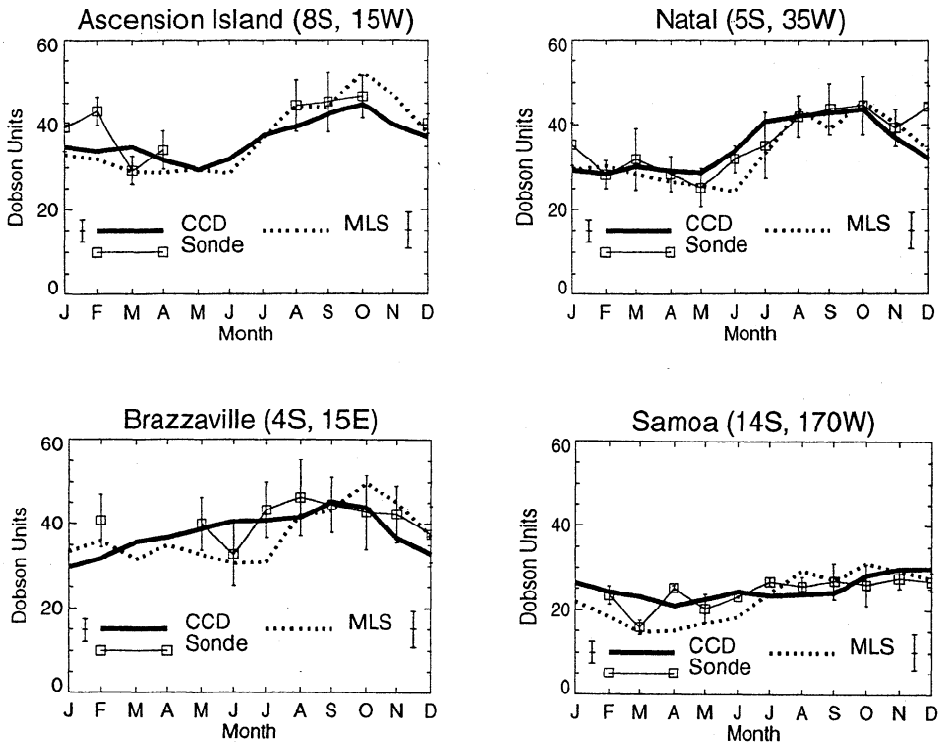

Figure 8. Monthly mean tropospheric column ozone at four southern tropical sonde stations from the CCD (bold), ozonesonde (boxes), and for completeness the assimilated UARS MLS/HALOE (dotted) methods. Seasonal cycles were derived by averaging all available data (EP TOMS not included). Included each month for the ozonesonde measurements are $\pm 1\sigma$ standard deviation bars. Monthly means from ozonesondes having fewer than five measurements within a given month are not plotted (see Table 1). Monthly 2σ errors for the CCD and MLS/HALOE climatologies, represented by the isolated vertical bars in the lower right and left portions of each frame, are estimated (see appendix) to be 2 and 4 DU, respectively.

the CCD and sonde data being distinctly different in both sampling and methodology.

In Figure 8 we compare the seasonal cycles at four southern tropical sonde stations from the CCD, ozonesonde, and (for completeness) the assimilated UARS MLS/HALOE method. The best agreement between all three measurements is perhaps at Natal. Samoa, located just east of the dateline in the eastern Pacific, shows smaller amounts and weaker seasonality compared to the other three south Atlantic stations. One might conclude that the CCD method compares slightly better with the ozonesondes, but it should be noted that the sondes have comparatively few measurements. For reference, Table 1 shows the number of ozonesonde profiles averaged together per month in Figure 8 to estimate 12-month seasonal cycles.

4.4. Interannual Variability in the Eastern Pacific

As a final example of the CCD method, Figure 9 shows January 1979 to December 1997 CCD 5° × 5° deseasonalized time series centered at equator, 147.5°W. In the top frame, $R > 0.9$ CCD stratospheric column ozone (bold) is plotted along with deseasonalized 30 hPa Singapore (1°N, 140°E) monthly mean zonal winds, showing a dominant quasi-biennial oscillation (QBO) in the ozone with persistent peak-to-peak amplitudes ~20 DU. This pattern is similar to the one derived from column ozone without subtracting the tropospheric component [e.g, *Chandra and Stolarski*, 1991]. In contrast, the bottom frame shows tropospheric column ozone plotted with the Southern Oscillation Index (SOI), indicating instead a dominant El Niño Southern

Table 1. Number of Available Ozonesonde Profile Measurements (1978-1996)

Station	Jan.	Feb.	March	April	May	June	July	Aug.	Sept.	Oct.	Nov.	Dec.
Ascension (8°S, 15°W)	6	5	5	7	4	0	2	5	10	14	2	6
Natal (5°S, 35°W)	19	12	15	20	13	11	25	18	29	31	25	15
Brazzaville (4°S, 15°E)	4	5	3	3	5	7	5	10	10	16	8	5
Samoa (14°S, 170°W)	3	14	8	8	15	12	14	19	19	18	14	13

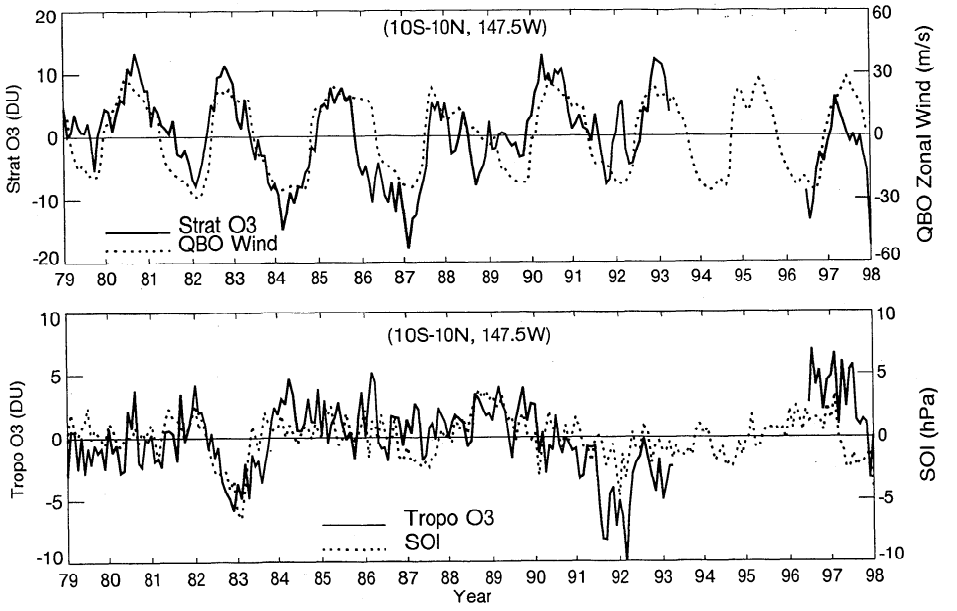

Figure 9. (top) Deseasonalized stratospheric column ozone (solid) for January 1979 through January 1998 using the CCD method, and deseasonalized 30 hPa Singapore zonal winds (dotted). The TOMS stratospheric column ozone time series was computed by averaging CCD above-cloud amounts between 120°E eastward to 120°W and between 10°S and 10°N (i.e., four separate time series). Deseasonalization was accomplished by subtracting 1979-1997 12-month climatologies. (bottom) Corresponding deseasonalized tropospheric ozone (solid) and coincident deseasonalized Southern Oscillation Index (SOI) time series (dotted). The SOI time series was generated from monthly-mean Tahiti (13°S, 131°E) minus Darwin (13°S, 150°W) sea level pressure differences obtained from the National Centers for Environmental Prediction (NCEP) Climate Prediction Center. Monthly 2σ errors for the CCD tropospheric column ozone time series are estimated (see appendix) to be 3.5 DU.

Oscillation (ENSO) in tropospheric ozone with reductions in column amount of around 5-10 DU during the ENSO events of 1982-1983 and 1991-1992. Reductions of 5-10 DU during these ENSO events are statistically significant in light of estimated 2σ monthly measurement errors of 3.5 DU (see appendix). The recent El Niño event of 1997-1998 also indicates a similar drop in tropospheric ozone during 1997, but slightly more positive by around 3-5 DU. The reason for the larger values may stem from calibration differences between Nimbus 7 and EP TOMS. (Calibration issues are beyond the scope of this investigation but remain an integral component of our ongoing improvement of the CCD technique.) We note that the sizeable reductions observed in tropospheric ozone during ENSO events indicates that a large portion of ENSO variability in total column ozone comes from the troposphere and not from within only a thin height range in the lower stratosphere (as stated by *Shiotani and Hasebe* [1994] using SAGE data). When SOI is low (El Niño), enhanced convection occurs in the tropical Pacific extending eastward across the dateline, conceivably vertically transporting low-value boundary layer ozone and reducing tropospheric column ozone. As shown by *Ziemke and Chandra* [1998a] most contribution to tropical tropospheric ozone variability including that of the tropical zonal wave 1 anomaly lies in the midtroposphere maximizing around 4-6 km altitude.

5. Summary

This study introduced two new methods for deriving tropospheric column ozone. In the first approach, stratospheric column ozone was determined by combining UARS HALOE and MLS ozone using simple regression. The HALOE data were used to extend the vertical span of MLS. It was demonstrated that the combination of these stratospheric ozone fields with TOMS total ozone can provide high-resolution maps of tropospheric column ozone. Generation of such detail is not possible from solar occultation measurements alone, such as from HALOE or SAGE.

We also investigated a new and promising CCD technique that yields tropospheric column ozone directly from TOMS high-density footprint measurements in regions of high tropopause-level clouds. The CCD method was shown to be capable of providing long time series (essentially late 1978 to the present) of distinctly stratospheric and tropospheric column ozone. In the tropical eastern Pacific on interannual timescales, the method indicated a dominant coupling of stratospheric ozone with the QBO and a dominant coupling of tropospheric ozone with El Niño events. This is a new result not shown before.

Both the CCD and assimilated UARS MLS/HALOE results were compared with ozonesonde data from sev-

eral southern tropical stations. Despite all of these three measurements being distinctly different in both sampling and technique, all three showed good qualitative aggreement. This study indicates that both the CCD and assimilated UARS MLS/HALOE methods are valid techniques that appear to work as well as previous approaches for determining local measurements of tropospheric column ozone in tropical latitudes. A main advantage of using the MLS/HALOE method over other residual methods is the horizontal resolution of measurements. The CCD technique has a distinct advantage over other methods (including the MLS/HALOE method) because it requires only TOMS measurements of total ozone and reflectivity. Potential regions for the CCD method include places not sampled by previous or current ground-based measurements. We note that in the absence of any other satellite ozone data source the TOMS CCD method can always directly provide long time series of tropospheric column ozone.

Although we have limited our analyses in this study to tropical latitudes, future applications of both the MLS/HALOE and CCD techniques will include the derivation of column ozone amounts in the extratropics. Regions most suitable for the CCD method include regions dominated by persistent high tropopause-level clouds, such as within or near the continents of North America, South America, and Asia.

Appendix: Error Analysis

Errors inherent to tropical tropospheric column ozone derived from the CCD method arise from three main sources. The first involves our first-order approximation of a zonally invariant stratospheric ozone column in the tropics. This assumption appears to have validity according to several previous studies that incorporated ozonesonde, HALOE, MLS, and SAGE ozone data [e.g., *Fishman and Larsen*, 1987; *Fishman et al.*, 1992; *Ziemke et al.*, 1996]. In relation to this, we note that the 2-day means plotted in Figure 5 indicated a relatively zonally invariant 0-100 hPa HALOE ozone column, but also present was a weak zonal wave structure with amplitude around 3-5 DU. Whether indeed this feature is real or not, local errors present in daily measurements of HALOE ozone mixing ratio may be larger than this. As discussed by *Brühl et al.* [1996], there are sizeable RMS errors in daily local measurements of HALOE ozone mixing ratio in the lower stratosphere, for example 18% at 40 hPa and 30% at 100 hPa. We can relate directly these errors to errors in computed stratospheric column ozone from HALOE. For example, ozonesonde measurements from Samoa in the tropical Pacific indicate ~25-30 DU column ozone year-round between 40 and 100 hPa, which translates to around 5-9 DU errors in stratospheric column measurements from HALOE. The accuracy of our first-order assumption of a zonally invariant stratospheric ozone column will require improved measurements of lower-stratospheric ozone. We note that the monthly averaging in this study reduces local measurement errors as well as natural zonal variabilities (~3-8 DU peak to peak) present in column ozone caused by shorter time-scale tropical normal modes, Kelvin and mixed Rossby-gravity waves [*Ziemke and Stanford*, 1994]. We anticipate that true zonal variability in monthly mean stratospheric ozone could be 5 DU.

A second source of error with the CCD method involves the natural variability of cloud top pressures for high-reflectivity cloud tops lying near the tropopause. Errors using the CCD technique will arise because high-reflectivity clouds seen by TOMS 360 and 380 nm ultraviolet measurements of reflectivity are not always associated with cloud tops at the tropopause. In determining potential cloud top error for the CCD method we first estimate a mean error in cloud top pressures and then use ozone and temperature sonde profiles to relate this error to ozone column abundance. The studies by *Eck et al.* [1987] and *Stowe et al.* [1988, 1989] directly compared TOMS reflectivity measurements with concurrent THIR cloud top temperatures at all latitudes, showing that the high-reflectivity TOMS measurement cases are indeed associated with high cloud tops near the tropopause. Our estimate of maximal cloud top pressure errors in the tropical Pacific using the results from these previous studies is anticipated to be ~50-100 hPa for the highest $R > 0.9$ reflectivity cases, with the largest pressure errors occurring for cloud tops lying below the tropopause. From these values we can then estimate resulting errors in column ozone from the CCD method by incorporating ozonesonde measurements. Sonde temperature and ozone profile data from tropical Pacific Samoa were used to estimate these expected errors. Linearization of sonde ozone mixing ratio about the measured tropopause pressure indicates that there will be on average ~1 DU error in CCD stratospheric column ozone for cloud top pressures varying 10 hPa from the tropopause pressure. Assuming 50-100 hPa CCD cloud top pressure variability of high-reflectivity cases in the tropical Pacific, the resulting errors in local measurements of stratospheric column ozone would then be around 5-10 DU. However, with the CCD method (see section 4.2) we average data from 120°E eastward across the dateline to 120°W (24 longitude grid points) at a given latitude to estimate the stratospheric column amount. During non-El Niño months there are few high-reflectivity cases in the eastern Pacific and including data east of the dateline to 120°W has little influence on derived tropospheric or stratospheric amounts (see Figure 6). During El Niño months there is an increase in convection in the eastern Pacific and the number of footprints available for the CCD method extends throughout the eastern and western Pacific. For either El Niño or non-El Niño months at least half (i.e., 12) of the grid points from 120°E to 120°W will contain data. An upper bound for the resulting error (standard error of the mean) of the stratospheric column amount then becomes $5/\sqrt{12}$ to $10/\sqrt{12}$ DU, that is, 2 to 3 DU.

In addition, there is a third source of error which arises because of the reduced efficiency of TOMS in de-

tecting variability of lower tropospheric ozone [*Hudson et al.*, 1995]. This results in about 1-3 DU further error in tropospheric ozone computed from the CCD method.

If we now assume independence of the three main error sources above, we can obtain an estimate of total error variance by summing these three variances. Taking upper-bounds in the variances then yields maximal local 2σ measurement errors of ~7 DU (i.e., $\sqrt{5^2+3^2+3^2}$ DU) on average for tropospheric ozone derived from the CCD method. This value for 2σ error applies to the local measurements plotted in Plate 2 and Figures 7 and 9. For Figure 8, 14 years were combined for determining seasonal cycle climatologies; local 2σ errors in this figure are estimated to be ~2 DU (i.e., $7/\sqrt{14}$ DU). The time series in Figure 9 was derived by averaging data between 10°S to 10°N (four separate time series). Monthly measurement errors in this figure are estimated to be ~3.5 DU (i.e., $7/\sqrt{4}$ DU).

For the MLS/HALOE regression method (as discussed in section 3), column ozone Ω_S in the stratosphere was derived from the single-parameter linear regression model $\Omega_S = \gamma\Omega_{0-46hPaMLS} + \epsilon$, where ϵ is the residual error and Ω_S in the regression is taken from HALOE overpass ozone (adjusted to tropopause pressure), relative to MLS. Coefficient γ was derived at each latitude by regressing daily gridded (24 longitude gridpoints at 5°latitude increments) stratospheric column ozone amounts from HALOE onto coincident 0-46 hPa MLS column ozone. Specifically, daily values for γ were derived as a function of latitude from $\gamma = \sum_{l=1}^{24} \Omega_S(l)\Omega_{0-46hPaMLS}(l) \;/\; \sum_{l=1}^{24} \Omega^2_{0-46hPaMLS}(l)$, where l is the longitudinal gridpoint index. These daily coefficients were then averaged over similar months from January 1993 through December 1996, resulting in a 12-month pseudoclimatology for γ. We note that the January 1993 starting date avoided most impact of aerosol contamination of HALOE ozone caused by the June 1991 eruption of Mt. Pinatubo. A standard multivariate linear model [e.g., *Guttman*, 1982] was applied to estimate errors in γ. It follows that the variance of γ is given by $\sigma^2_\gamma = \sigma^2/\sum_{l=1}^{24} \Omega^2_{0-46hPaMLS}$, where σ^2 is estimated from $\sum_{l=1}^{24} \epsilon^2(l)/23$.

As Figure 1 showed, 2σ uncertainties for the regression coefficients were ~1% of 0-46 hPa MLS column ozone amounts, or ~2 DU (1% of 200 DU). This is small compared to intercalibration errors resulting from combining TOMS with MLS and HALOE, and also the interpretation of tropopause pressure from NCEP analyses. Local errors in tropopause pressure of 20 hPa translate to only around 2 DU error using Samoa data (discussed above) but errors are larger, ~3-5 DU in the Atlantic region from similar analyses done for Natal, Brazzaville, and Ascension Island sonde data. Additional errors result after differencing the final MLS/HALOE regression product with TOMS because these two fields are not intercalibrated. Estimated local errors in residual tropospheric ozone from this may likely exceed 6-8 DU. Again assuming independence between these potential sources of error, summation of maximum error variances results in ~10 DU (i.e., $\sqrt{2^2+5^2+8^2}$ DU) estimated maximal local 2σ measurement errors for the MLS/HALOE method. This value for 2σ applies to local measurements shown in Plate 1 and Figure 2. For Figure 8, 7 years were included for climatological estimates of local seasonal cycles; local 2σ errors in Figure 8 are estimated to be ~4 DU (i.e., $10/\sqrt{7}$ DU).

Acknowledgments. We appreciate greatly the efforts of the members of the NASA TOMS Nimbus Experiment and Information Processing Teams in producing the extensive TOMS version 7 data. We wish to thank S. J. Oltmans for providing ozonesonde data from Samoa, C. J. Seftor for help on obtaining the level 2 TOMS footprint data, and D. Larko for providing statistical data for ISCCP cloud top pressures. In addition, we want to thank J. L. Stanford, R. D. Hudson, A. M. Thompson, and the two anonymous referees for helpful comments in improving this manuscript.

References

Brühl, et al., Halogen Occultation Experiment ozone channel validation, *J. Geophys. Res., 101*, 10,217–10,240, 1996.

Chandra, S., and R. S. Stolarski, Recent trends in stratospheric ozone: Implications of dynamical and El Chichon perturbations, *Geophys. Res. Lett., 18*, 2277-2280, 1991.

Eck, T. F., P. K. Bhartia, P. H. Hwang, and L. L. Stowe, Reflectivity of Earth's surface and clouds in ultraviolet from satellite observations, *J. Geophys. Res., 92*, 4287–4296, 1987.

Fishman, J., and J. C. Larsen, Distribution of total ozone and stratospheric ozone in the tropics: Implications for the distribution of tropospheric ozone, *J. Geophys. Res., 92*, 6627–6634, 1987.

Fishman, J., V. G. Brackett, and K. Fakhruzzaman, Distribution of tropospheric ozone in the tropics from satellite and ozonesonde measurements, *J. Atmos. Terr. Phys., 54*, 589–597, 1992.

Fishman, J., V. G. Brackett, E. V. Browell, and W. B. Grant, Tropospheric ozone derived from TOMS/SBUV measurements during TRACE A, *J. Geophys. Res., 101*, 24,069–24,082, 1996.

Froidevaux, L., et al., Validation of UARS Microwave Limb Sounder ozone measurements, *J. Geophys. Res., 101*, 10,017–10,060, 1996.

Guttman, I., *Linear Models, An Introduction*, 358 pp., Wiley-Interscience, New York, 1982.

Hudson, R. D., J.-H. Kim, and A. M. Thompson, On the derivation of tropospheric column ozone from radiances measured by the total ozone mapping spectrometer, *J. Geophys. Res., 100*, 11,137–11,145, 1995.

Hudson, R. D., and A. M. Thompson, Tropical tropospheric ozone (TTO) from TOMS by a modified-residual method, *J. Geophys. Res.*, in press, 1998.

Jacob, J., et al., Origin of ozone and NO_x in the tropical troposphere: A photochemical analysis of aircraft observations over the South Atlantic basin, *J. Geophys. Res., 101*, 24,235–24,250, 1996.

Kim, J. H., R. D. Hudson, and A. M. Thompson, A new method of deriving time-averaged tropospheric column ozone over the tropics using TOMS radiances: Intercomparison and analysis, *J. Geophys. Res., 101*, 24,317–24,330, 1996.

Krishnamurti, T. N, H. E. Fuelberg, M. C. Sinha, D. Oosterhof, E. L. Bensman, and V. B. Kumar, The meteorological environment of the tropospheric ozone maximum over the tropical South Atlantic Ocean, *J. Geophys. Res., 98*, 10,621–10,641, 1993.

Krishnamurti, T. N., M. C. Sinha, M. Kanamitsu, D. Oosterhof, H. Fuelberg, R. Chatfield, D. J. Jacob, and J. Logan, Passive tracer transports relevant to the TRACE A Experiment, *J. Geophys. Res., 101*, 23,889–23,907, 1996.

McPeters, R. D., et al., Nimbus-7 total ozone mapping spectrometer (TOMS) data products user's guide, *NASA Ref. Publ. RP-1384*, 67 pp., 1996.

Rossow, W.B., and L.C. Garder, Validation of ISCCP cloud detections, *J. Clim., 6*, 2370–2393, 1993.

Shiotani, M., and F. Hasebe, Stratospheric ozone variations in the equatorial region as seen in stratospheric aerosol and gas experiment data, *J. Geophys. Res., 99*, 14,575–14584, 1994.

Stowe, L. L., et al., Nimbus-7 global cloud climatology. Part I: Algorithms and validation, *J. Clim., 1*, 445–470, 1988.

Stowe, L. L., et al., Nimbus-7 global cloud climatology. Part II: First year results, *J. Clim., 2*, 671–709, 1989.

Thompson, A. M., K. E. Pickering, D. P. McNamara, M. R. Schoeberl, R. D. Hudson, J. H. Kim, E. V. Browell, V. W. J. II. Kirchhoff, and D. Nganga, Where did tropospheric ozone over southern Africa and the tropical Atlantic come from in October 1992? Insights from TOMS, GTE/TRACE-A and SAFARI-92, *J. Geophys. Res., 101*, 24,251–24,278, 1996.

Vukovich, F. M., V. Brackett, J. Fishman, and J. E. Sickles, II, On the feasibility of using the tropospheric ozone residual (TOR) for non-climatological studies on a quasi-global scale, *J. Geophys. Res., 101*, 9093–9105, 1996.

Ziemke, J. R., and S. Chandra, On tropospheric ozone and the tropical wave 1 in total column ozone, *Proc. 18th Quadrenn. Ozone Symp.*, in press, 1998a.

Ziemke, J. R., and S. Chandra, Comment on "Tropospheric ozone derived from TOMS/SBUV measurements during TRACE A" by J. Fishman et al., *J. Geophys. Res., 103* 13,903–13,906, 1998b.

Ziemke, J. R., and J. L. Stanford, The quasi-biennial oscillation and tropical waves in total ozone. *J. Geophys. Res., 99*, 23,041–23,056, 1994.

Ziemke, J. R., S. Chandra, A. M. Thompson, and D. P. McNamara, Zonal asymmetries in southern hemisphere column ozone: Implications of biomass burning, *J. Geophys. Res., 101*, 14,421–14,427, 1996.

P. K. Bhartia and S. Chandra, NASA Goddard Space Flight Center, Chemistry and Dynamics Branch, Code 916, Greenbelt, MD 20771. (e-mail: bhartia@carioca.gsfc.nasa.gov, chandra@chapman.gsfc.nasa.gov)

J. R. Ziemke, Software Corporation of America, Lanham, MD 20706. (e-mail: ziemke@jwocky.gsfc.nasa.gov)

(Received November 7, 1997; revised May 4, 1998; accepted May 7 1998.)